One-Step Controllable Synthesis for High-Quality Ultrafine Metal Oxide Semiconductor Nanocrystals via a Separated Two-Phase Hydrolysis Reaction

ARTICLE *in* JOURNAL OF THE AMERICAN CHEMICAL SOCIETY · MARCH 2008

Impact Factor: 12.11 · DOI: 10.1021/ja0778702 · Source: PubMed

9 AUTHORS, INCLUDING:

Wenfu Yan
Jilin University
145 PUBLICATIONS **2,297** CITATIONS
SEE PROFILE

Weimin Yang
Beijing Research Institute of Chemical Industry
40 PUBLICATIONS **816** CITATIONS
SEE PROFILE

Zaiku Xie
China Petroleum and Chemical Corporation
82 PUBLICATIONS **1,325** CITATIONS
SEE PROFILE

Taolei Sun
Wuhan University of Technology
69 PUBLICATIONS **4,075** CITATIONS
SEE PROFILE

J|A|C|S
ARTICLES
Published on Web 02/07/2008

One-Step Controllable Synthesis for High-Quality Ultrafine Metal Oxide Semiconductor Nanocrystals via a Separated Two-Phase Hydrolysis Reaction

Kangjian Tang,[†,‡] Jianan Zhang,[||] Wenfu Yan,[||] Zhonghua Li,[||] Yangdong Wang,[‡] Weimin Yang,[‡] Zaiku Xie,[‡] Taolei Sun,*[,†,§] and Harald Fuchs[†,§]

Physikalisches Institut, Muenster University, Muenster 48149, Germany, Center for Nanotechnology, Muenster 48151, Germany, Shanghai Research Institute of Petrochemical Technology, SINOPEC, Shanghai 201208, P. R. China, and State Key Laboratory of Inorganic Synthesis and Preparative Chemistry, College of Chemistry, Jilin University, Changchun 130012 P.R. China

Received October 31, 2007; E-mail: Sunt@uni-mienster.de

Abstract: A one-step synthesis method is described to prepare high-quality ultrafine inorganic semiconductor nanocrystals via a two-phase interface hydrolysis reaction under hydrothermal conditions. With the synthesis of ZrO_2 quantum dots as an example, we show that the prepared nanocrystals have good monodispersity and high crystallinity, as well as other related superior properties, e.g., strong photoluminescence and excellent photocatalytic activities. Also the crystal size can be conveniently adjusted in the range below 10 nm through controlling the reaction temperature. Besides that, this method also shows other distinct advantages compared with other methods reported previously. First, the preparation process is simple and cheap and does not contain any complicated posttreatment procedure. Second, products (without coating) can be collected from the organic phase which effectively avoids grain aggregation induced by the capillary concentration in the water environment. Third, the production yield is very high (almost 100%) and the organic and water phases after reaction can be easily recycled for next reaction. Therefore, it provides a promising strategy for the large-scale industrial production of different kinds of high-quality inorganic nanocrystals.

Introduction

Inorganic semiconductor nanocrystals[1−3] have attracted great interest in recent decades due to their importance in a wide variety of applications including photocatalysis,[4−6] electric devices,[7] light-emitting devices,[8,9] solar cells,[10] bioimaging, biosensors,[11,12] etc. Although numerous methods have been developed to fabricate these kinds of materials,[13] such as the sol technique,[14,15] micelles or emulsion method,[16] sol−gel process,[17,18] hydrothermal synthesis,[19,20] pyrolysis,[21,22] chemical vapor deposition,[23] etc., they usually suffer from complicated preparation and posttreatment procedures or problems of aggregation or poor monodispersity, which greatly influence their properties and restrict their large-scale production and successful applications in industry. Simple methods that are suitable for industrial production to prepare monodispersed semiconductor nanocrystals with tunable size (especially under 10 nm) still remain a big challenge.

[†] Muenster University.
[‡] SINOPEC.
[§] Center for Nanotechnology.
[||] Jilin University.

(1) Wang, Y.; Herron, N. *J. Phys. Chem.* **1991**, *95*, 525−532.
(2) Fernandez-Garcia, M.; Martinez-Arias, A.; Hanson, J. C.; Rodriguez, J. A. *Chem. Rev.* **2004**, *104*, 4063−4104.
(3) Kong, X. Y.; Ding, Y.; Yang, R.; Wang, Z. L. *Science* **2004**, *303*, 1348−1351.
(4) Kalyanasundaram, K. *Photochemistry in Microheterogeneous Systems*; Academic Press: New York, 1987.
(5) Gratzel, M. *Heterogeneous Photochemical Electron Transfer*; CRC Press: Boca Raton, FL, 1989.
(6) Lewis, L. N. *Chem. Rev.* **1993**, *93*, 2693−2730.
(7) Kamat, P. V.; Meisel, D. *Semiconductor Nanoclusters-Physical, Chemical, and Catalytic Aspects*; Elsevier Science: New York, 1997.
(8) Wang, Y. *Acc. Chem. Res.* **1991**, *24*, 133−139.
(9) Gaponik, N. P.; Talapin, D. V.; Rogach, A. L. *Phys. Chem. Chem. Phys.* **1999**, *1*, 1787−1789.
(10) Gur, I.; Fromer, N. A.; Geier, M. L.; Alivisatos, A. P. *Science* **2005**, *310*, 462−465.
(11) Bruchez, M.; Moronne, M.; Gin, P.; Weiss, S.; Alivisatos, A. P. *Science* **1998**, *281*, 2013−2016.
(12) Alivisatos, A. P.; Gu, W.; Larabell, C. *Annu. Rev. Biol. Eng.* **2005**, *7*, 55−76.
(13) Burda, C.; Chen, X.; Narayanan, R.; El-Sayed, M. A. *Chem. Rev.* **2005**, *105*, 1025−1102.
(14) Murray, C. B.; Norris, D. J.; Bawendi, M. G. *J. Am. Chem. Soc.* **1993**, *115*, 8706−8715.
(15) Yin, M.; O'Brien, S. *J. Am. Chem. Soc.* **2003**, *125*, 10180−10186.
(16) Murray, C. B.; Norris, D. J.; Bawendi, M. G. *J. Am. Chem. Soc.* **1993**, *115*, 8706−8715.
(17) Li, Y.; White, T.; Lim, S. H. *Rev. Adv. Mater. Sci.* **2003**, *5*, 211−215.
(18) Mondelaers, D.; Vanhoyland, G.; Van den Rul, H.; D'Haen, J.; Van Bael, M. K.; Mullens, J.; Van Poucke, L. C. *Mater. Res. Bull.* **2002**, *37*, 901−914.
(19) Wang, X.; Zhuang, J.; Peng, Q.; Li, Y. *Nature* **2005**, *437*, 121−124.
(20) Liao, Q. L.; Tannenbaum, R.; Wang, Z. L. *J. Phys. Chem. B* **2006**, *110*, 14262−14265.
(21) Depero, L. E.; Bonzi, P.; Musci, M.; Casale, C. J. *Solid State Chem.* **1994**, *111*, 247−252.
(22) Li, W.; Gao, L.; Guo, J. *Nanostruct. Mater.* **1998**, *10*, 1043−1049.
(23) Gao, P.; Ding, Y.; Wang, Z. *Nano Lett.* **2003**, *3*, 1315−1320.
(24) Parthasarathy, R.; Martin, C. R. *Nature* **1994**, *369*, 298−301.
(25) Miao, Z.; Xu, D.; Ouyang, J.; Guo, G.; Zhao, X.; Tang, Y. *Nano Lett.* **2002**, *2*, 717−720.

10.1021/ja0778702 CCC: $40.75

Scheme 1. Diagram for the Preparation Process with ZrO_2 as an Example[a]

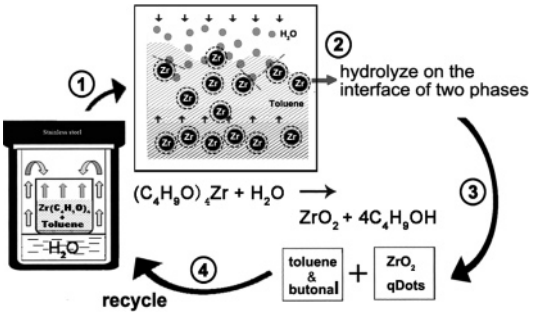

[a] Key: (1) Evaporation and diffusion of two phases in the autoclave is shown. (2) Hydrolysis reaction occurs at the interface area of two phases. (3) Shown are zro$_2$ qdots formation and crystallization by the hydrolysis and hydrothermal reactions, which will mainly deposit into the organic phase. (4) After the separation of solid products, the organic phase could be easily recycled for the next reaction by the fractionation method.

In this contribution, we report a novel simple one-step controllable preparation method for high-quality ultrafine metal oxide semiconductor nanocrystals via the two-phase hydrolysis reaction under hydrothermal conditions. With an example of sub-10 nm ZrO_2 quantum dots (qdots), we show that the products have good monodispersity and high crystallinity, as well as other related superior properties, e.g., strong photoluminescence, excellent photocatalytic activities, etc. More interestingly, the crystal size can be conveniently adjusted in the range below 10 nm through controlling the reaction temperature. Besides that, this method also shows other distinct advantages compared with other methods reported previously. First, the preparation process is simple and cheap and does not contain any complicated posttreatment procedure. Second, products (without coating) can be collected from the organic phase which effectively avoids grain aggregation induced by the capillary concentration in water environment. Third, the production yield is very high (almost 100%) and the organic and water phases after reaction can be easily recycled for the next reaction. It would be especially beneficial for industrial production and help to largely reduce production costs. Therefore, it provides a promising strategy for large-scale industrial production of different kinds of high-quality inorganic nanocrystals, provided that an appropriate two-phase reaction can be found.

Results and Discussion

The essence of our method is the combination of the interface hydrolysis and nucleation process in the confined nanoscale organic matrix and the crystallization process under hydrothermal conditions. Scheme 1 shows the preparation process of ZrO_2 qdots as an example. The water phase and the organic phase (toluene, bp 110 °C) containing a metal alkyl oxide precursor ($Zr(OC_4H_9)_4$ (TBZ)) were placed separately in the same Teflon-lined hydrothermal chamber. Under hydrothermal temperatures (100−240 °C), the water and organic phases are much different from those at normal conditions because of the autogenous high pressure when the temperature exceeds the boiling points of water and toluene. It is a nonliquid and nongas state, and the two phases may exist as tiny droplets that diffuse gradually to the other side to form an interface. The hydrolysis reaction between TBZ and water will occur immediately when the water and toluene droplets meet and collide with each other, and the crystal nucleus will form simultaneously in this way. At the same time, the hydrothermal conditions also provides a stable environment for further crystallization.

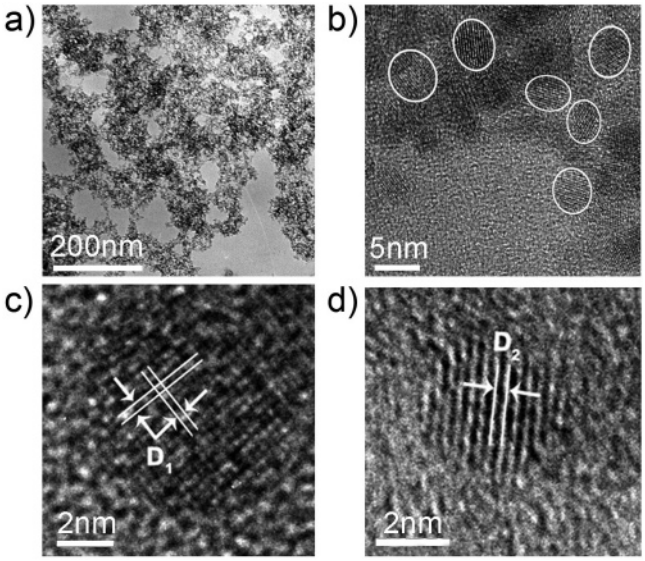

Figure 1. (a) Low-resolution TEM and (b) corresponding high-resolution TEM images of ZrO_2 qdots prepared at 160 °C. Further magnified images show the coexistence of the (c) tetragonal and (d) monoclinic ZrO_2 qdots in the samples.

The tiny toluene droplets can act as nanoreactors with uniform sizes which confine the further growth of the nanocrystals. It is a dynamic process that the droplet sizes and the collisions between different droplets largely depend on the reaction temperature. Therefore, it provides a convenient approach to control the nanocrystal size through adjusting the reaction temperature. The nanocrystals will deposit in the organic phase because toluene has a higher boiling point than water and thus the interface may locate at the organic phase side. The separation of the water and organic phases can efficiently prevent further growth of the nanocrystals during the remaining hydrothermal period because the hydrolysis reaction can only occur at the interface area, which is especially helpful to prepare the monodispersed ultrafine (e.g., <10 nm) nanocrystals.

Product Characterizations. The ZrO_2 samples collected from the organic phase are all fine white powders with a yield higher than 99.9% (only very small amount (less than 0.1%) of product can be found in water phase). ^{1}H NMR (Supporting Information Figure S1) study reveals that there is no unreacted TBZ and only an amount of *n*-butanol (the resultant of the hydrolysis reaction) exists in the organic phase, indicating that the reaction is very complete. And the chemical analysis on the organic and water phases further shows that there is only a trace amount of water in the organic phase and negligible toluene in the water phase. The above obsevations show that the resultant solutions can be easily recycled for the next reaction, and thus, this method is environmental friendly and has great potential for large-scale production in industry.

Figure 1a shows the typical transmission electron microscope (TEM) image for a product prepared with hydrothermal temperature of 160 °C. The product shows excellent dispersity although there is no organic coating (as the reaction system only contains the reactant, water, and toluene) on the particle surface. This is much different from the phenomena observed for other methods to prepare the uncoated inorganic nanocrystals, in which serious aggregation will usually be observed due to the

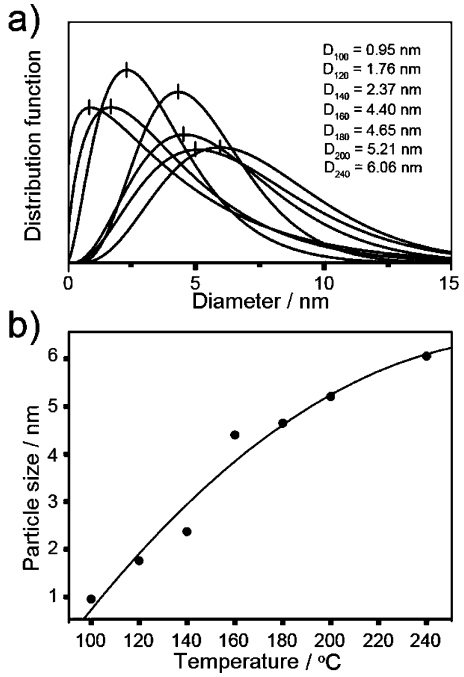

Figure 2. (a) Size distribution function of ZrO_2 qdots that calculated from the SAXS data. (b) Relationship between the particle size (maximum probability of diameter) and the hydrothermal temperature.

capillary condensation induced by water evaporation. This reveals that the collection in a suitable organic phase may serve as an efficient strategy to solve such a kind of problem. The corresponding high-resolution TEM image (Figure 1b) shows that the samples are well crystallized round qdots with good monodispersity and particle size of ~4.4 nm, the crystal lattice of which can be clearly observed in further magnified images (Figure 1c,d). Meanwhile, the orthogonal lattice ($D_1 \approx 0.296$ nm, Figure 1c) and the parallel lattice ($D_2 \approx 0.318$ nm, Figure 1d) for different particles can be indexed to the (111) plane of the tetragonal and the $(\bar{1}11)$ plane of the monoclinic ZrO_2 structure, respectively. This implies the coexistence of the tetragonal and monoclinic ZrO_2 qdots in the samples.

The particle sizes of the ZrO_2 qdots prepared under different hydrothermal temperatures were further investigated by the small-angle X-ray scattering (SAXS) technique.[26] The curves of the distribution function (Figure 2a) that calculated from the SAXS patterns (see Supporting Information) show a good monodispersity for all the samples that were prepared at different temperatures, and their average sizes increase monotonously from ~1.0 to ~6.1 nm when the temperature increases from 110 to 240 °C (Figure 2b).

This indicates an excellent controllability over the grain size of the nanocrystals through adjusting the reaction temperature, which may be due to the thermodynamic reasons of the hydrolysis reaction. To confirm this effect, we used the same method to prepare TiO_2 nanocrystals (precursor: $Ti(OC_4H_9)_4$), which show good crystallinity and monodispersity similar to those of the ZrO_2 material reported above. The grain size also increases regularly from ~6.7 to ~22.1 nm (Table 1) when the reaction temperature changes from 100 to 220 °C. As indicated by the X-ray line profile analysis (Supporting Information Figure S2), the as-prepared TiO_2 nanocrystals have approximate sizes

Table 1. Average Sizes of the TiO_2 Nanocrystals Prepared at Different Temperatures

	D([*hkl*][a]/nm				
temp/°C	[101]	[200]	[105]	[211]	av size/nm
100	7.0	5.9	8.0	6.0	6.7
120	10.9	8.0	10.0	7.0	8.9
140	14.2	13.9	13.9	12.2	13.5
180	15.5	15.7	17.3	15.5	16.0
220	20.9	22.6	24.3	20.7	22.1

[a] D is the size in different crystal dimensions [*hkl*] that calculated from the profile analysis of the corresponding powder XRD peaks (see Supporting Information).

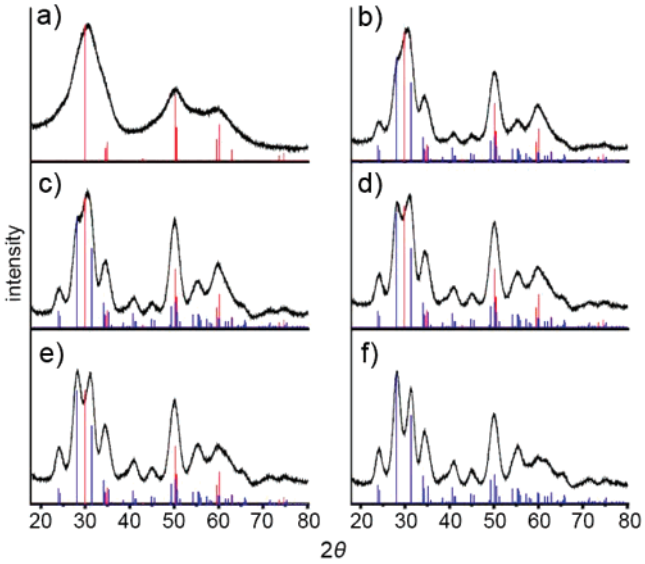

Figure 3. XRD patterns for ZrO_2 qdots that were prepared at different temperatures: (a) 100 °C; (b) 120 °C; (c) 140 °C; (d) 160 °C; (e) 180 °C; (f) 200 °C. Red lines: characteristic peaks for the tetragonal phase. Blue lines: characteristic peaks for the monoclinic phase.

at different dimensions (e.g., [101], [200], [105], [211]; see Table 1), indicating a proximately spherical morphology of the nanocrystals.

The crystallinity is further investigated by powder X-ray diffraction (XRD) measurement (Figure 3), in which characteristic peaks of monoclinic ZrO_2 can all be found in the XRD patterns for different samples. At the same time, the broadening and the overlapping of the 2θ peaks after 30° also cover all the typical peaks of the tetragonal phase. Although the tetragonal phase is thermodynamically unstable at room temperature, and the corresponding bulk material can only exist at a temperature higher than 1170 °C, Garvie[27] theoretically predicted that pure tetragonal ZrO_2 can be stable at room temperature when the particle size is less than 30 nm.[28] Therefore, these data also support the existence of the tetragonal ZrO_2 qdots. It can also be observed that the products prepared at 100 °C show very broad XRD peaks, which may be because of the very small particle size (the nanocrystals can only be called as quasi-crystal), and the peaks become much sharper with the increase of the preparation temperature, indicating an crystallinity increase with the increase of the crystal size. Further analysis of the XRD patterns indicates that the samples prepared at 100 °C (Figure 3a) and 110 °C are mainly composed of

(26) Schomaker, V.; Glauber, R. *Nature* **1952**, 290−291.

(27) Garvie, R. C. *J. Phys. Chem.* **1978**, *82*, 218−224.
(28) Xie, S.; Iglesia, E.; Bell, A. T. *Chem. Mater.* **2000**, *12*, 2442−2447.

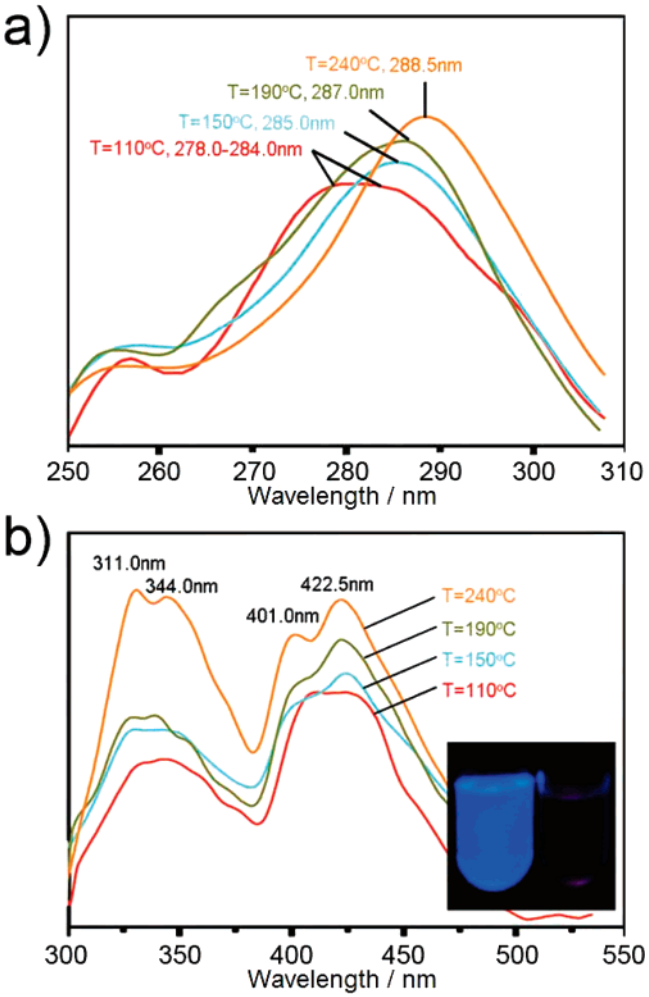

Figure 4. Fluorescence spectra of the ZrO_2 qdots prepared at different temperatures (T) and dispersed in chloroform: (a) excitation spectra, in which an obvious red-shift of the absorption peaks can be observed; (b) emission spectra (excitation wavelength: 285 nm). Four main peaks located at 331, 344, 401, and 423 nm in the blue-light region can be observed. Inset: blue-light emission of ZrO_2 qdots dispersed in chloroform (recorded by a CCD camera in a dark room, irradiated by a black-light lamp (365 nm)) (left tube, with ZrO_2 qdots; right tube, without ZrO_2 qdots).

tetragonal ZrO_2 nanocrystals, and there is almost no monoclinic phase because of the lack of the corresponding characteristic peaks before 30°. However, the characteristic peaks of the monoclinic phase begin to appear at 120 °C and their relative intensities increase with the increase of preparation temperature, indicating the appearance and the content increase of the monoclinic nanocrystals.[29,30] For samples prepared at temperatures higher than 200 °C (Figure 3f), the monoclinic phase becomes the main component and the content of the tetragonal phase is very small, which is consistent with the high-resolution TEM observation. This indicates an interesting nanosize-dependent phase transition from tetragonal to monoclinic nanocrystals at low temperatures, which will be examined in detail in further research.

Photoluminescent and Photocatalytic Activities of the Samples. ZrO_2[30] is a classic material that has been widely applied in many industrial fields, such as advanced ceramics technology,[31] etc. Moreover, as an n-type semiconductor, it is also widely used as photocatalyst in photochemical reactions, such as photocatalytic oxidation of propene, photoreduction of carbon dioxide, etc.,[33,34] and the nanosized particles are reported to possess excellent properties because of the large specific surface area and other effects.[35,36] When the size decreases to a value that is comparable to the Bohr exciton radius of the material, e.g., 10 nm or less, it will exhibit some unique properties because of the nanosize effect, such as photoluminescence, etc. To check the performance of the as-prepared ZrO_2 qdots, the luminescent and photocatalytic properties were further investigated. As shown in the excitation spectra (Figure 4a), the absorption peaks for the ZrO_2 qdots exhibit obvious red-shift from ~278.0−284.0 to ~288.5 nm when the size of the qdots increases from ~ 1.0 nm (prepared at T = 110 °C) to ~6.1 nm (T = 240 °C), indicating a distinct quantum size effect. The emission spectra (Figure 4b) show four emission peaks in the blue light region for all the samples. As a result, strong blue light emission (inset of Figure 4b) when samples are irradiated by a UV-light lamp (365 nm) can be clearly observed even at daytime. These features are related to the near band-edge transitions and a midgap trap state that results from incomplete surface passivation such as surface defects and oxygen vacancies,[15,37] and the change of the corresponding band gap with the decrease of the nanocrystal size.

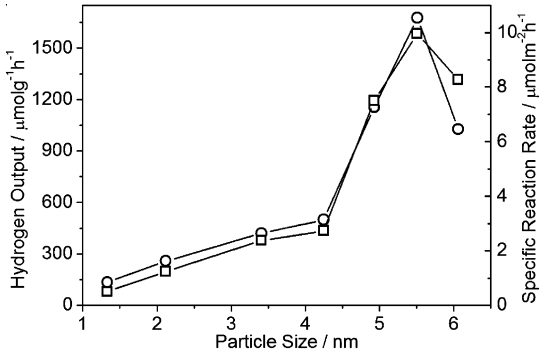

Figure 5. Photocatalytic properties of the ZrO_2 qdots with different particle sizes: (○) hydrogen output efficiency; (□) specific reaction rate considering the specific surface area of the nanocrystals.

Significantly, the as-prepared ZrO_2 qdots also show excellent and size-dependent photocatalytic activity. Figure 5 shows the relationship between the particle size and the photocatalytic efficiency of the ZrO_2 qdots (as denoted by the hydrogen output in the photocatalytic hydrogen production experiment). It can be observed that the photocatalytic efficiency increases first with the increase of crystal size and reaches a maximum value of 1676 μmol·g^{-1}·h^{-1} at the size of ~5.5 nm (prepared at 210 °C) and then decreases dramatically when the size increases further. Because the specific surface area (SSA) is an important factor influencing the photocatalytic efficiency, we measured the SSA values of the samples prepared at different temperatures. As shown in Table 2, the SSA values increase significantly

(29) Noh, H.-J.; Seo, S.-S.; Kim, H.; Lee, J.-K. *Mater. Lett.* **2003**, *57*, 2425−2431.
(30) Zhao, N.; Pan, D.; Nie, W.; Ji, X. *J. Am. Chem. Soc.* **2006**, *128*, 10118−10124.
(31) Cahn, R. W. *Nature* **1988**, *332*, 112−113.
(32) Corma, A. *Chem. Rev.* **1995**, *95*, 559−614.
(33) Witko, M. *J. Mol. Catal.* **1991**, *70*, 277−333.
(34) Wang, C.-M.; Fan, K.-N.; Liu, Z.-P. *J. Am. Chem. Soc.* **2007**, *129*, 2642−2647.
(35) Edelstein, A. S.; Cammaratra, R. C. *Nanomaterials: Synthesis, Properties and Applications*; Institute of Physics Publishing: London, 1998.
(36) Sun, T.; Tan, H.; Han, D.; Fu, Q.; Jiang, L. *Small* **2005**, *1*, 959−963.
(37) Liang, J.; Deng, Z.; Jiang, X.; Li, F.; Li, Y. *Inorg. Chem.* **2002**, *41*, 3602−3604.

Table 2. Average Particle Size and Specific Surface Area (BET) of the ZrO_2 Nanocrystals Prepared at Different Temperatures

	temp/°C						
param	110	130	150	170	190	210	240
av particle size/nm	1.3	2.1	3.4	4.3	4.9	5.5	6.1
specific surf area/ $m^2 g^{-1}$	273.3	209.1	177.3	182.8	153.8	168.3	124.1

with the decrease of the reaction temperatures.[38] The specific reaction rate of the photocatalytic reaction after considering the SSA values is also included in Figure 5. It can be observed that 5.5 nm also shows the highest specific reaction rate, which indicates that the crystallinity is another important factor influencing the photocatalytic efficiency of ZrO_2 nanocrystals. To make a comparison, we further investigated the photocatalytic activity of the commercial ZrO_2 (Beijing Chemical Plant, Beijing, China) and TiO_2 (p25, Degussa) powders, which show hydrogen output efficiencies of about 673 and 300 μmol·$g^{-1}h^{-1}$, respectively. This indicates that the as-prepared ZrO_2 qdots have excellent photocatalytic activity that are much superior to that of the the commercial products.

Conclusions

In summary, a simple one-step synthesis method is described to fabricate high-quality metal oxide semiconductor nanocrystals via a two-phase interface hydrolysis reaction under hydrothermal conditions. Due to the confined nucleation and the hydrothermal crystallization processes, as well as the advantages of the interface reaction, which efficiently prevents the further growth of the crystals, we show that this method is very suitable to prepare monodispersed, highly crystallized, ultrafine (typically 10 nm or less) nanocrystals. The collection in the organic phase can efficiently prevent nanocrystal aggregation, although there is no organic coating on their surface. The size of the nanocrystals can be conveniently adjusted through controlling the reaction temperature. Moreover, other advantages, e.g., simple and low cost, high production yield, highly recyclable reaction solutions, etc., make them easy to be industrialized. It is also considered that this method can be easily extended to the synthesis of other high-quality inorganic nanocrystals, e.g., metals,[39] metal sulfides, metal selenides,[40] etc., if only suitable interface reactions could be found.

Acknowledgment. We thank the partially financial support from the SINOPEC and the Federal Ministry of Education and Research of Germany (BMBF).

Supporting Information Available: Experimental details, ^{1}-HNMR analysis of the organic phase after reaction, calculation method for the size distribution function of ZrO_2 qdots by SAXS analysis, and XRD patterns of the TiO_2 nanocrystals. This material is available free of charge via the Internet at http://pubs.acs.org.

JA0778702

(38) Kawaguchi, H. *Prog. Polym. Sci.* **2000**, *25*, 1171−1210.
(39) Jana, N. R.; Peng, X. *J. Am. Chem. Soc.* **2003**, *125*, 14280−14281.
(40) Pradha, N.; Xu, H.; Peng, X. *Nano Lett.* **2006**, *6*, 720−724.